

The influence of atmospheric circulation types on regional patterns of precipitation in Marmara (NW Turkey)

H. Baltacı^{1,2} · T. Kindap¹ · A. Ünal¹ · M. Karaca¹

Received: 11 June 2015 / Accepted: 25 September 2015 / Published online: 9 October 2015
© Springer-Verlag Wien 2015

Abstract In this study, regional patterns of precipitation in Marmara are described for the first time by means of Ward's hierarchical cluster analysis. Daily values of winter precipitation data based on 19 meteorological stations were used for the period from 1960 to 2012. Five clusters of coherent zones were determined, namely Black Sea-Marmara, Black Sea, Marmara, Thrace, and Aegean sub-regions. To investigate the prevailing atmospheric circulation types (CTs) that cause precipitation occurrence and intensity in these five different rainfall sub-basins, objective Lamb weather type (LWT) methodology was applied to National Centers of Environmental Prediction (NCEP)/National Center for Atmospheric Research (NCAR) reanalysis of daily mean sea level pressure (MSLP) data. Precipitation occurrence suggested that wet CTs (i.e. N, NE, NW, and C) offer a high chance of precipitation in all sub-regions. For the eastern (western) part of the region, the high probability of rainfall occurrence is shown under the influence of E (SE, S, SW) atmospheric CTs. In terms of precipitation intensity, N and C CTs had the highest positive gradients in all the sub-basins of the Marmara. In addition, although Marmara and Black Sea sub-regions have the highest daily rainfall potential during NE types, high daily rainfall totals are recorded in all sub-regions except the Black Sea during NW types.

1 Introduction

One of the most significant issues in climate sciences is understanding the characteristics of rainfall and its spatio-temporal variability in a region because of its social and economic implications (Collier and Krzysztofowicz 2000 and references therein). Accordingly, many researchers have attempted to cluster rainfall regions (e.g. Fovell and Fovell 1993; Gong and Richman 1995), and their relationship with large-scale circulations (e.g. Lopez-Bustins et al. 2008; Ning and Bradley 2015) or circulation types (CTs) (e.g. Huth et al. 2008; Philipp et al. 2010) on defined regional, national or global scales.

Numerous studies have endeavoured to classify climate zones and atmospheric CTs of Turkey and its regions. In terms of climate zones, Erinç (1984) qualitatively described seven climate regions by taking into account climatic differences and the changes in the social and economic properties of the country, which are still used for describing the classifications of climate regions. Türkeş (1996) quantitatively characterised climate zones by applying a coefficient of variations to the two primary climatological variables (i.e. temperature and precipitation). Subsequently, Ünal et al. (2003) investigated the climate regions of Turkey by using hierarchical clustering techniques. They first compared five cluster methods, including single, complete, centroid and average linkage as well as Ward's methodologies. They found that Ward's method gave better results and found seven different climate zones and six precipitation regions. Türkeş and Tatlı (2011) identified eight consistent precipitation regime regions for the Anatolian Peninsula using spectral clustering for investigating atmospheric and geographical controls.

Sönmez and Kömüçü (2011) reclassified the rainfall regions of Turkey by using non-hierarchical K-means methodology and the relationship between drier or wetter periods and

✉ H. Baltacı
baltacihakki@gmail.com

¹ Eurasia Institute of Earth Sciences, Istanbul Technical University, Maslak, 34469 Istanbul, Turkey

² Turkish State Meteorological Service, Kütükçü Alibey Caddesi No.4, 06120 Ankara, Turkey

the North Atlantic Oscillation (NAO). They found six rainfall clusters, which included Aegean and Marmara regions in the same cluster, and determined that temporally dry periods are partially explained by NAO. Differently from previous studies, Sahin and Cigizoglu (2012), using the Ward's and neuro-fuzzy method, investigated the sub-climate and sub-regional precipitation characteristics as well as main climate and precipitation regions together with the physical properties of the regions. According to the results, Turkey is composed of seven main precipitation climates and 16 sub-regional precipitation climates.

In terms of atmospheric CTs, Baltacı et al. (2015) detected composites and frequencies of CTs as well as their contribution to the seasonal daily mean precipitation for every station in the Marmara region (NW Turkey). To this end, an objective version of the Lamb weather type (LWT) methodology, which is commonly described in the literature, was applied to National Centers of Environmental Prediction (NCEP)/National Center for Atmospheric Research (NCAR) reanalysis of daily mean sea level pressure data (MSLP). They calculated the seasonal contribution of each CT to the daily precipitation amounts for 21 meteorological stations without considering the influence of CTs on sub-regional precipitation.

Some of the previous cluster analysis solutions revealed that the Marmara and Aegean regions have the same precipitation climate and are likely to be one cluster. However, besides highly spatial and temporal rainfall variability between these two regions, the spatial distribution of precipitation characteristics of Marmara shows different behaviour. Non-uniform spatial and temporal distribution of the rainfall in Marmara and its sub-basins, which is the most populated region and the economic powerhouse of Turkey, influences the infrastructure (e.g. flash floods), limited or unrestricted fresh water storage in water basins, and the socioeconomic development of the region and country. Therefore, more comprehensive studies for understanding the regional patterns of precipitation in Marmara are required and should also consider its synoptic perspectives.

In addition to quantifying the intra-annual daily mean precipitation amounts for every CT at each station (Baltacı et al., 2015), this study explores which CTs quantitatively cause precipitation occurrence and intensity in the sub-basins of the Marmara region. For this purpose, as a first step, Ward's method clustering technique was adapted to the winter precipitation records (wettest season) of 19 land-based meteorological stations for the period from 1960 to 2012. In terms of CTs, the LWT methodology was used for the same period. CTs and their contribution to the precipitation occurrences and their amounts under each sub-basin were investigated using two indices.

In Section 2, a description of the climatological and synoptic characteristics of the study area, along with the data and the methods used, is provided. The results of the cluster and LWT

analysis are presented in Section 3. Section 4 provides conclusions.

2 Data and methodology

2.1 Climatological and synoptic characteristics of the Marmara region

The Marmara region exhibits the properties of a transition climate between Black Sea and Mediterranean climates together with its own characteristics. Compared with the Black Sea precipitation characteristics, lower rainfall values are recorded for the whole year. Compared with the Mediterranean precipitation regime, Marmara receives more precipitation during the year. The region is surrounded by water bodies (i.e. the Aegean Sea and the Black Sea in Fig. 1), and the transfer of humidity from these seas by atmospheric circulations plays a dominant role in all seasons. The cyclones over Genoa and Iceland affect the region on particular time scales. When the Genoa low-pressure centre (LPC) moves towards Marmara, more precipitation and humidity are transferred to the inner parts of the region. In terms of Icelandic LPC, the cyclones move from the Balkan Peninsula to the region and, while passing over the Istranca Mountains, deposit their moisture over the Balkan countries and bring dry air to the Marmara region. In some summer months, a low Asiatic monsoon (Türkeş and Tatlı 2011) extends from the south of the country to the inner parts of the region and drier and hotter atmospheric conditions together with daily maximum temperature peaks are observed. General wind directions are north-northeast because of the activity of the pressure systems, and therefore, the Black Sea plays a significant role in determining the air-sea interactions and moisture transport. The sea effect mechanism creates snowfall (extreme rainfall) events and threatens social life, causing economic losses, especially in winter (fall) months. During the spring and fall seasons, convectivity and its associated unpredicted precipitation episodes appear in the land areas of the Marmara region. A very mountainous area is located in the south-southeast part of the region. A plateau basin is positioned in the northwest of the region (Thrace basin) with low altitudes (Table 1). High mountain borderlines (i.e. Istranca and Mt Uludağ (2543 m)) cause rain shadows over the particular sub-basins, and rapid urbanisation and deforestation threaten the limited water basins of the region. Moreover, the high variability of the cyclone frequencies seen in the region, especially in the winter, the most significant season for heavy rainfall, gives us a solid basis from which to describe the spatio-temporal distribution of the precipitation values, focusing on sub-regional precipitation.

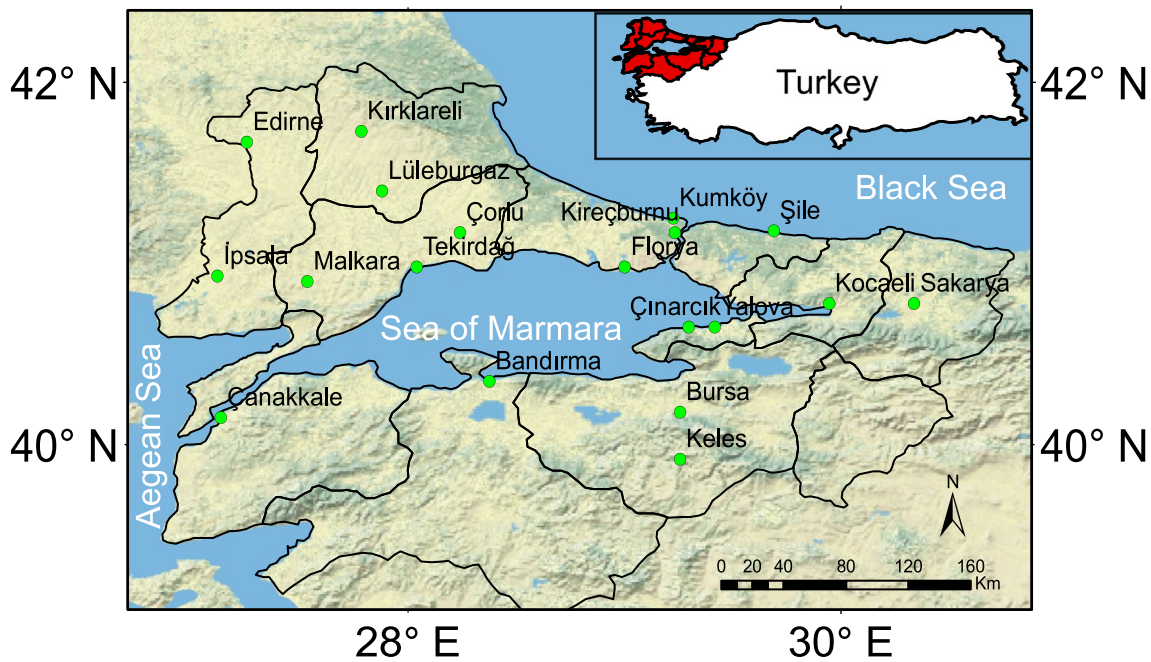


Fig. 1 The Marmara region and meteorological stations used in this analysis, which are described in Table 1. The *inset* shows the location of the region in Turkey

2.2 Spatial and temporal precipitation variability

We focused on the spatial and temporal variability of winter precipitation totals, vital for the sustainability of water management policies. In our study, we utilised all available long-

term climatological data, which registered at 19 homogenised meteorological stations to better represent the region. Daily precipitation values of winter months were provided by the State Meteorological Service of Turkey for the period between 1960 and 2012. In order to understand the spatial distribution

Table 1 Geographic coordinates, altitudes, and the DJF precipitation characteristics of the stations for the period from 1960 to 2012

Station name	Latitude (N)	Longitude (E)	Altitude (m)	DJF precipitation (mm)	Contribution to MAP (%)	DJF wet days (>0 mm)	DJF thresholds (mm)
Bandırma	40.35	27.97	58	299.3	41.6	46	49.0
Bursa	40.18	29.07	100	267.3	38.3	43	37.7
Çanakkale	40.15	26.42	6	271.5	44.1	35	47.8
Çınarcık	40.65	29.12	20	314.0	35.8	44	51.9
Çorlu	41.17	27.80	183	193.8	33.8	44	30.9
Edirne	41.67	26.57	51	185.3	31.4	36	36.5
Florya	40.98	28.75	36	255.0	39.3	46	32.0
İpsala	40.93	26.40	10	224.9	35.9	33	42.8
Keles	39.92	29.07	1063	295.0	39.2	44	40.8
Kireçburnu	41.17	29.04	58	312.7	37.7	51	35.5
Kırklareli	41.73	27.23	232	178.9	31.9	32	42.0
Kocaeli	40.78	29.93	76	277.2	34.3	50	35.2
Kumköy	41.25	29.03	30	298.1	36.7	47	41.2
Lüleburgaz	41.40	27.35	46	179.3	31.1	27	37.3
Malkara	40.90	26.92	283	248.6	36.1	34	41.1
Sakarya	40.78	30.42	31	275.5	32.9	46	31.2
Şile	41.18	29.61	31	300.0	35.5	49	42.0
Tekirdağ	40.98	27.55	4	206.6	35.3	35	37.5
Yalova	40.65	29.27	4	282.3	37.7	45	38.8

of wintertime precipitation over the years, its average percentage contribution to mean annual precipitation (MAP), the average number of wet days and threshold values according to the T10 method (Osborn et al. 2000; Burt and Ferranti 2012) were extracted for 19 stations. The T10 threshold was defined for each station separately, which is the daily rainfall amount that corresponds to the top 10 % of ranked cumulative rainfall for the reference period (1960–2012). It is shown in Table 1 that the lowest winter rainfall totals are recorded for the NW part of the region, which is the agricultural basin (e.g. Kırklareli, Lüleburgaz, Edirne). Highest winter rainfalls are shown for seaside stations close to the Marmara Sea and the Black Sea (e.g. Şile, Çınarcık, Kireçburnu). The percentage contribution of winter (DJF) precipitation to the MAP changes from 31.1 to 44.1 % in the Marmara stations. Every other day produces rainfall located in the north and northeast part of the studied area. Interestingly, although DJF rainfall totals are minimal at Kırklareli, threshold values dropped to 42 mm. This indicates that the magnitude of the daily precipitation is higher than that of the neighbouring stations.

In order to understand the temporal behaviour of the winter mean precipitation for the region, weighted averages of DJF precipitation totals and their annual anomalies were calculated using data for the 19 meteorological stations. As shown in Fig. 2, the three driest periods occurred during 1972, 1989, and 1992, respectively. On the other hand, the three wettest periods occurred in 1963, 1981, and 2010, respectively. According to the 10-year moving average, a sharp decrease in DJF precipitation can be observed during the late 1970s, followed by an increasing trend in the 1980s. From the late 1990s to today, an increasing trend of precipitation can be observed in the region.

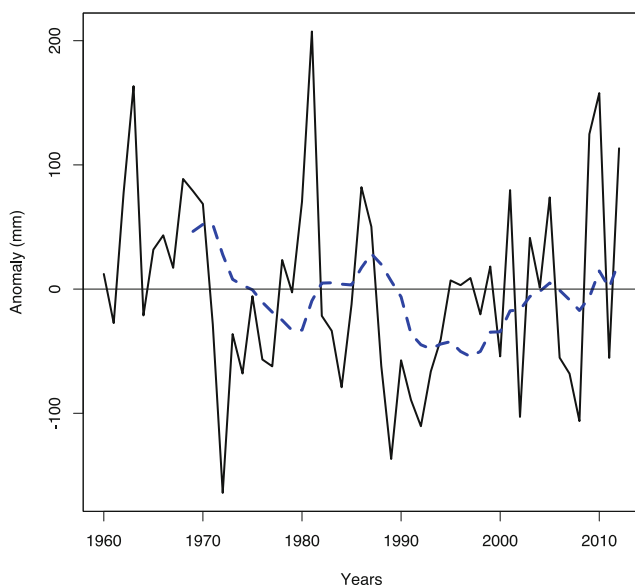


Fig. 2 Winter (DJF) precipitation anomalies of Marmara for the period from 1960 to 2012. Dashed lines indicate the 10-year moving average

2.3 Atmospheric circulation classifications

In order to determine the synoptic classifications, an objective version of the LWT (Jenkinson and Collison 1977; Jones et al. 1993) methodology was applied to the daily MSLP data derived by NCEP/NCAR reanalysis (Kalnay et al. 1996) for 1960 to 2012. As a result of the calculation of flow and vorticity terms of the method, 27 different CTs were identified: 8 directional (north (N), northeast (NE), east (E), southeast (SE), south (S), southwest (SW), west (W), northwest (NW)), 16 hybrid (combination of directional and non-directional types), and 3 pure types (cyclonic (C), anticyclonic, and unclassified (U)). The grid resolution and location and the indices' formulas were adapted from Baltacı et al. (2015).

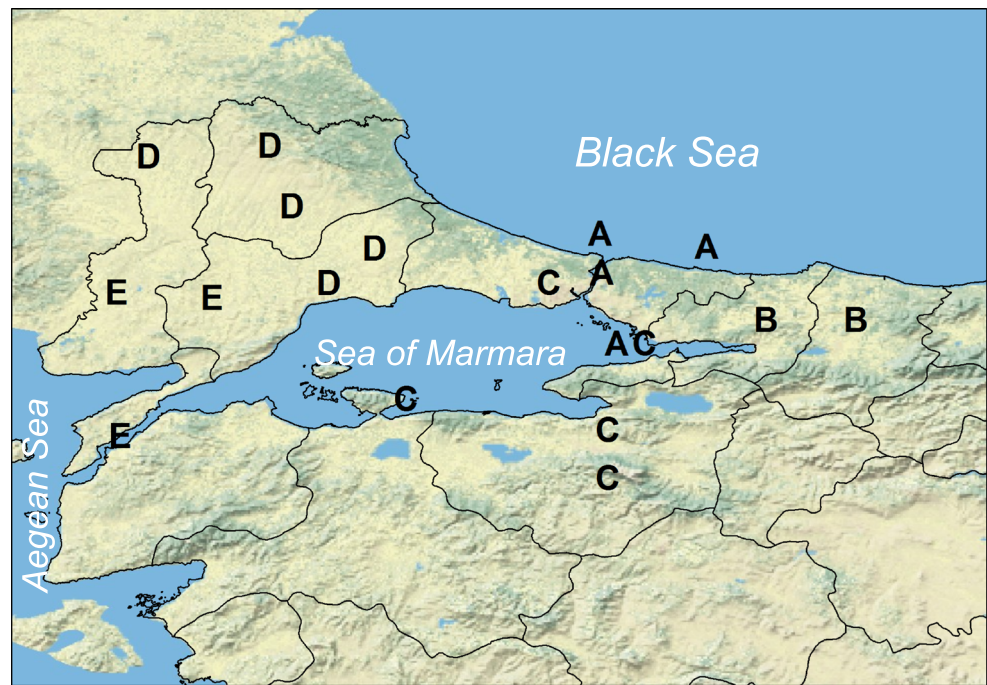
3 Results and discussion

3.1 Regional patterns of precipitation in Marmara

We preferred Ward's methodology for detecting sub-regional precipitation of Marmara, as it is both widely used and is actually the most suitable method (Ünal et al. 2003) for describing the climate regions of Turkey. To standardise the winter precipitation values based on 19 meteorological stations, zero mean and unit variance were used. The dissimilarity was measured by Euclidean distance. As a result of the clustering solutions, five clusters were considered sufficient for our region, even though the objective method for identifying the number of clusters to be retained was not universally accepted (Fig. 3 and Table 2).

Later, to obtain statistical information for each rainfall cluster, a box-whisker plot of the clusters was devised (Fig. 4), where the central mark on each box is the median, the edges of the box are the 25th and 75th percentiles, and the dashed lines extending to the most extreme data are the whiskers. For each box, the outliers and the means are plotted with "o" and "+" symbols, respectively. Cluster A includes four stations and shows similar characteristics to the Black Sea and Marmara Sea regions. This sub-region has the highest average DJF rainfall (308 mm). Maximum DJF precipitation occurred during 1981 with 780 mm. In cluster B, two stations indicate Black Sea region rainfall properties; the winter rainfall average increased to 277 mm. For cluster C, four of five stations are located close to the Sea of Marmara and present a typical Marmara precipitation climate (Fig. 3). The second highest winter precipitation is observed in this cluster with 282 mm (Fig. 4). In terms of cluster D, five land-based stations located NW of Marmara have the lowest winter average precipitation total of 193 mm (Figs. 3 and 4). This sub-region is known as the Thrace basin and has great importance in terms of agricultural production (e.g. rice and sunflowers). Three stations in the west part of the Marmara region are separated from the

Fig. 3 The five clusters of the Marmara region according to Ward's method. The cluster letters are explained in Table 2



Thrace basin and typically present an Aegean rainfall climate. In this cluster, E, the average winter precipitation is 257 mm.

3.2 Atmospheric circulation classifications

The most frequent atmospheric CTs were investigated for the Marmara region. As shown in Table 3, 93 % of the winter mean frequencies of CTs relates to the eight directional and two vorticity types (C and A). For this reason, the long-term winter composites of 10 CTs (out of 27) were taken into account (Fig. 5). Despite the low frequency of northerly types (N), maximum daily precipitation amounts are recorded in the A, B, and C clusters. This N type is the second wettest type after cyclonic (C) patterns for D and E sub-regions (Table 3) because there is no humidity transfer for the D and E regions (Fig. 5). The rainfall contribution to the winter total is between 5 and 7 % for the eastern parts of the region (A, B, and C), but the ratio decreases 3 % in the cluster E sub-basin. In north-easterly (NE) cases (the second most frequent CT over Marmara), the maximum daily precipitation values are

observed close to the Black Sea stations (cluster B), followed by clusters A and C with values of 6.68 and 5.84 mm/day, respectively. Percentage contribution to the winter rainfall of NE types are 34.74, 28.02, 26.71, 14.47, and 14.09 % in B, A, C, D, and E sub-regions, respectively. In this type, the region is under the influence of a high-pressure centre (HPC) located over eastern Europe and a low-pressure centre (LPC) located over Cyprus; hence, NE types bring humidity from the semi-closed water body called the Black Sea (Fig. 5). In the most frequent CTs (easterly (E) types), although the sub-regions have low daily precipitation values, the percentage addition to winter rainfall total changes from 19.75 to 28.28 % for the D and A clusters, respectively. The position of HPC over the Balkan Peninsula and clockwise rotation result in easterly patterns in Marmara (Fig. 5). The flows move over Marmara and more winter rainfall records are observed in the Thrace basin and the Aegean region (clusters D and E in Table 3). Both the daily rainfall intensity and the average number of rainfalls decrease during the active southeasterly (SE) and southerly (S) patterns (Table 3). In these cases, as a consequence of

Table 2 Clustering results of winter precipitation records based on 19 meteorological stations together with their sub-regional names for the period from 1960 to 2012

Cluster letter	No. of stations and their names	Definition
A	4 (Kireçburnu, Kumköy, Şile, and Çınarcık)	Marmara and Black Sea regions
B	2 (Kocaeli and Sakarya)	Black Sea region
C	5 (Bursa, Yalova, Keles, Bandırma, and Florya)	Marmara region
D	5 (Edime, Kırklareli, Lüleburgaz, Çorlu, and Tekirdağ)	Thrace region
E	3 (Çanakkale, İpsala, and Malkara)	Aegean region

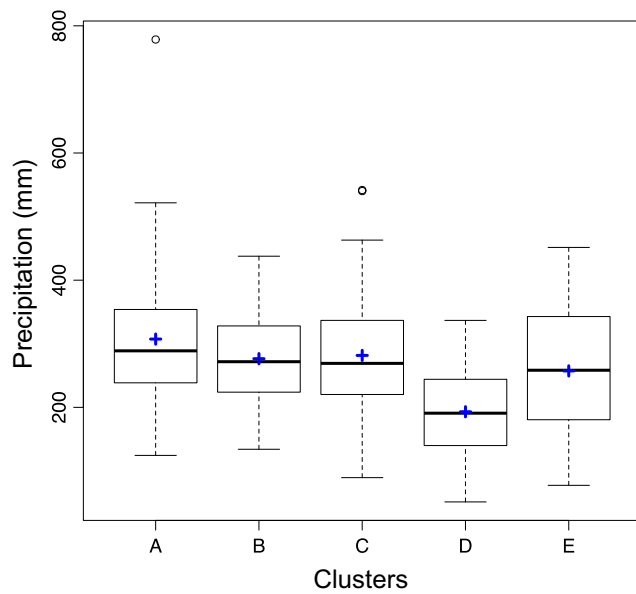


Fig. 4 Box-plot of the Ward's method clusters for the 1960–2012 period. Cluster letters are explained in Table 2

the Genoa LPC and HPC over the north of the Caspian Sea, the flows move throughout the eastern Mediterranean and leave precipitation before reaching the Taurus mountains, which divide the Mediterranean coastal region of southern Turkey from the central Anatolian plateau. Therefore, the areas behind the mountains have a rain shadow character (Fig. 5). When the HPC shifts south of the Caspian Sea, the pattern turns into southwesterly (SW) types, and the impact of the Genoa LPC can be seen in the region. Humidity is transferred throughout the western Mediterranean to the Marmara region without any geographic obstacles such as mountains. Every 10th CT occurs in this type. The highest daily rainfall total applies to the D and E clusters. Average numbers of westerly types increase up to 13.69 %, and the contribution to winter rainfall is at its maximum in the western parts of the

Fig. 5 Long-term wintertime daily mean sea level pressure (MSLP) composites of each of the eight main directional and two vorticity CTs during the period from 1960 to 2012. The red rectangle indicates the Marmara region. H and L mark the high and low-pressure centres, respectively

region. Similar synoptic conditions, like N cases, are shown during northwesterly (NW) patterns. Compared with N types, the NW patterns bring partly dry air from the Balkan countries, and hence, lower daily precipitation values are recorded in the whole of Marmara. In cyclonic (C) types (the fifth most frequent CT), an LPC is located over Marmara, daily rainfall total increases to 7.18 and 9.34 mm and is the wettest CT for the D and E clusters, respectively. During anticyclonic (A) types, an HPC is located over Marmara and has the lowest daily rainfall potential of all sub-regions.

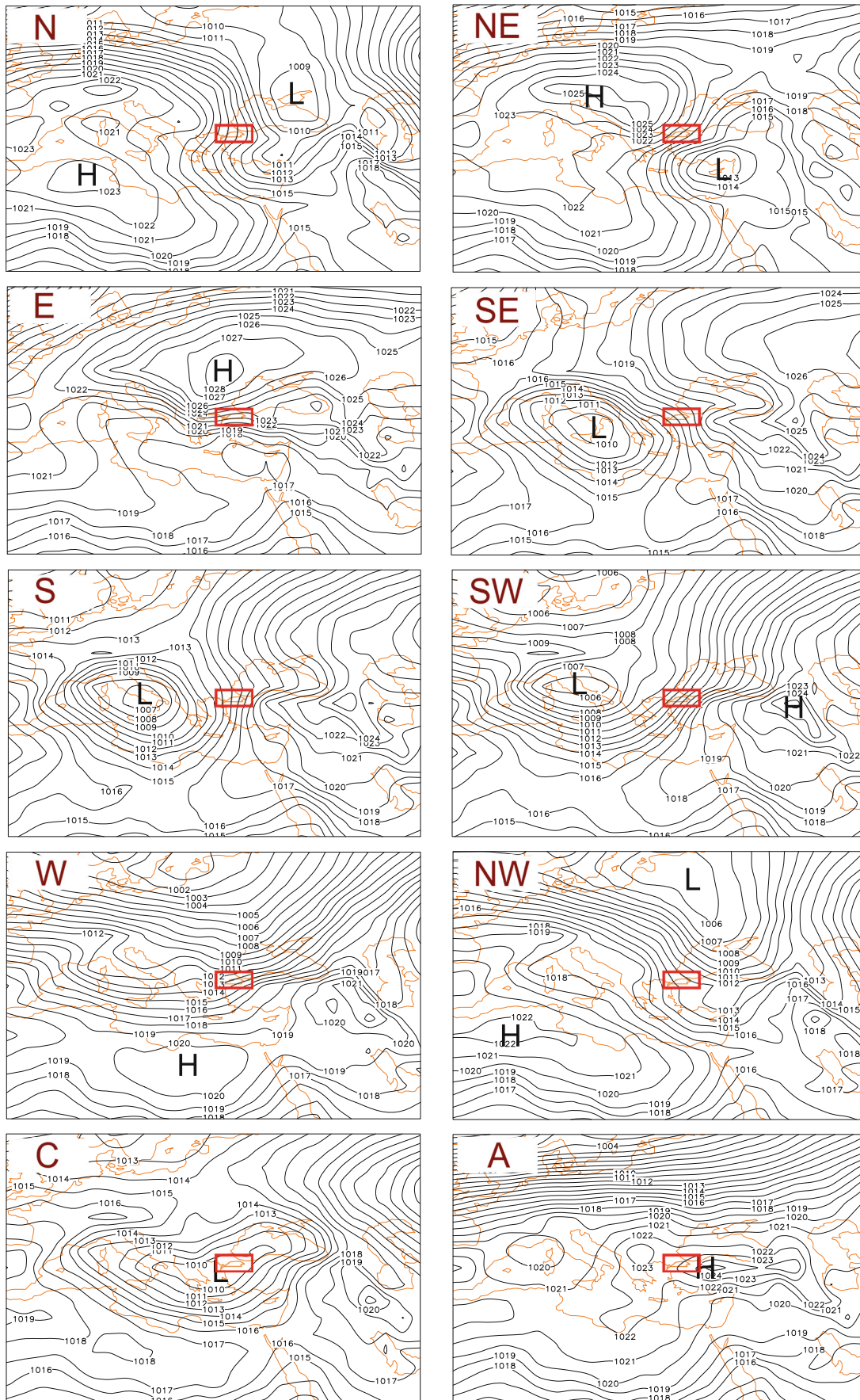
3.3 Precipitation occurrence and amount

Precipitation occurrence of each CT is derived from the daily rainfall totals. A wet day is defined when the daily total precipitation is greater than or equal to 1 mm. In the study, the probability of having a wet day for each CT and cluster was analysed. As seen in Fig. 6, the wettest days are shown as N, NE, NW, and C types. In terms of N patterns, the highest probability of having a wet day was observed in the north and northeast part of the region. The probability ratio decreases to 57 % west and northwest of the Marmara region. In NE cases, the chance of having wet days is much more distinct between north-northeast and west-northwest areas of the region. In spite of the low frequencies of NW types, 70 % of the patterns result in a wet day in clusters A, B, and C. In cyclonic conditions, observed frequencies of wet days are almost 70 % in the four clusters (except cluster B).

Although N, NE, NW, and C types result in a high probability of rainy conditions in winter months, their frequencies

Table 3 Winter (DJF) mean frequencies of CTs and their contribution to the daily mean precipitation amounts (mm day⁻¹) and to total precipitation (%) for the defined five clusters during the period from 1960 to 2012

CTs	%day	A		B		C		D		E	
		mm/day	% tot P	mm/day	% tot P	mm/day	% tot P	mm/day	% tot P	mm/day	% tot P
N	1.63	11.49	5.50	11.47	6.10	11.84	6.19	5.13	3.91	5.83	3.33
NE	14.28	6.68	28.02	7.46	34.74	5.84	26.71	2.17	14.47	2.81	14.09
E	29.58	3.26	28.28	2.75	26.57	2.48	23.48	1.43	19.75	2.27	23.60
SE	3.91	1.55	1.78	0.97	1.23	1.38	1.73	1.79	3.27	3.00	4.12
S	3.30	1.78	1.73	1.53	1.65	1.86	1.97	2.02	3.11	2.69	3.11
SW	9.99	1.08	3.17	0.71	2.33	1.25	4.00	2.11	9.85	3.08	10.79
W	13.69	2.22	8.91	1.82	8.13	2.43	10.67	2.18	13.98	2.35	11.30
NW	1.86	6.39	3.49	4.78	2.90	6.84	4.08	5.06	4.40	5.24	3.42
C	4.58	6.83	9.18	4.18	6.24	7.18	10.54	7.18	15.37	9.34	14.99
A	8.13	1.26	3.01	1.48	3.92	1.12	2.93	0.46	1.74	0.54	1.55



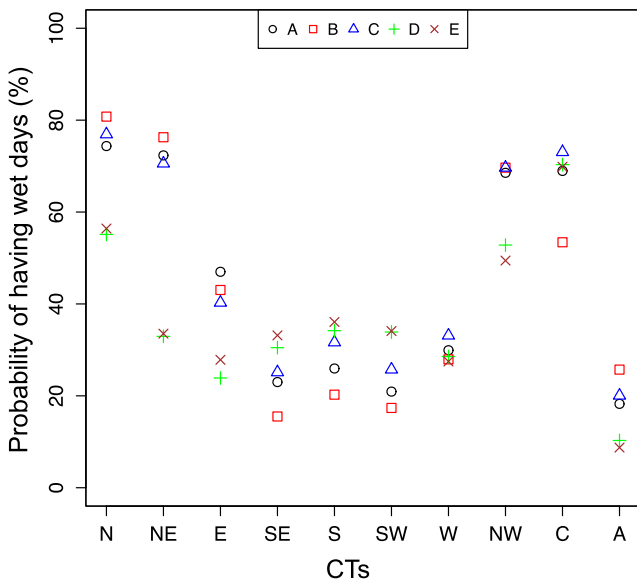


Fig. 6 The probability of having a wet day for the directional and two vorticity CTs for the five sub-basins (cluster letters A, B, C, D, and E)

(22.5 % in Table 3) and their contribution to total rainfall (average 43.5 % in Table 3) cannot give enough detailed information to explain the rainfall characteristics of the region. Therefore, we explored the chances of rainfall occurrence and intensity during each CT and cluster by using two index calculations.

3.4 Spatial variability of precipitation

Two indices were defined and applied to the Iberian rainfall to determine the role of each CT in precipitation occurrence and amount (Goodess and Jones 2002). Brisson et al. (2011) also applied these indices to the limited number of stations to characterise different precipitation regions in Belgium. The first index was termed the

normalised relative occurrence of rainy days (by the ratio $PROB_{ct}/PROB_{tot}$) and the formula is as follows:

$$\frac{PROB_{ct}}{PROB_{tot}} = \frac{N_{wet_{ct}} \cdot N_{tot}}{N_{ct} \cdot N_{wet_{tot}}}, \tag{1}$$

where $N_{wet_{ct}}$ and N_{ct} are the total number of wet days (≥ 1 mm) and total number of days within the CT. N_{tot} and $N_{wet_{tot}}$ are as the total number of days and the total number of wet days within the entire period (53 years).

The second index was used to describe positive or negative anomalies based on the intensity of precipitation during CT, which was termed normalised relative daily intensity of ($PREC_{ct}/PREC_{tot}$) and can be written as follows:

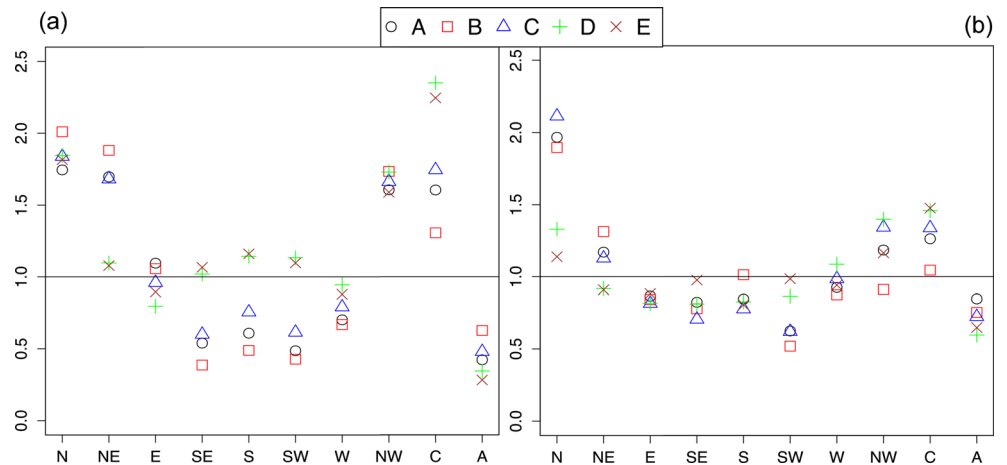
$$\frac{PREC_{ct}}{PREC_{tot}} = \frac{TAR_{ct} \cdot N_{wet_{tot}}}{N_{wet_{ct}} \cdot TAR_{tot}}, \tag{2}$$

where TAR_{ct} is the total accumulation of rain during the wet days of a specific CT, $N_{wet_{ct}}$ is the total number of wet days within the CT, $N_{wet_{tot}}$ is the total number of wet days, and TAR_{tot} is the total accumulation of rain during the wet days of the 53-year period.

If index values of $PROB_{ct}/PROB_{tot}$ were higher (lower) than 1, this implied a positive (negative) anomaly, which causes a high (low) chance of precipitation occurrence compared with the average of all CTs. An index $PREC_{ct}/PREC_{tot}$ higher (lower) than 1 indicated that the intensity of rainfall on a wet day is larger (smaller) than the average intensity on a wet day during the entire period.

According to the results for the normalised relative occurrence of rainy days ($PROB_{ct}/PROB_{tot}$), wet CTs (N, NE, NW, and C) indicate a high chance of precipitation in all sub-regions of the Marmara (Fig. 7a). On the other hand, southerly components of the patterns (i.e. SE, S, and SW) have a high chance of rainy days appearing in the western parts of the region (clusters D and E). In addition, in E types, the high

Fig. 7 **a** The normalised relative occurrence of rainy days per CT ($PROB_{ct}/PROB_{tot}$) and **b** the normalised relative daily intensity of precipitation per CT ($PREC_{ct}/PREC_{tot}$) for each cluster and CT. Circle, square, triangle, plus, and multiplication signs mark the sub-regional precipitation marked by cluster letters A, B, C, D, and E, respectively.



chance of wet days is more evident in the east of the region (clusters A and B) compared with the other clusters. The lowest precipitation occurrence of rainy days is shown during the A patterns in the whole of Marmara.

Based on the $PREC_{ct}/PREC_{tot}$ results, the highest precipitation intensity gradients occur during the N and C types in the whole domain (Fig. 7b). For NE cases, the high rainfall intensity of wet days is shown in the Marmara-Black Sea, Black Sea, and Marmara sub-basins (i.e. A, B, and C clusters) of the studied area. During NW types, high rainfall magnitude affects all Marmara except the stations close to the Black Sea (cluster B).

3.5 Rainfall magnitude categories

To explore the CTs that cause intense precipitation (see Section 3.3), we comprehensively analysed the daily intensity of precipitation during particular CTs. For this reason, the classification of daily rainfall magnitude (PRCP) in previous works was adopted (Osborn et al. 2000; Osborn and Hulme 2002; Gallego et al. 2006). We constructed five categories of rainfall magnitude: no rain, light rain ($0 \text{ mm} < \text{PRCP} < 3 \text{ mm}$), moderate rain ($3 \text{ mm} < \text{PRCP} < 9 \text{ mm}$), intense rain ($9 \text{ mm} < \text{PRCP} < 21 \text{ mm}$), and very intense rain ($>21 \text{ mm}$). Percentage contributions of N and C CTs to the rainfall magnitude were analysed for five clusters. As one can see from Fig. 8a, every other day of the northerly types produced intense and very intense precipitation in the A, B, and C clusters. The distribution of the moderate and intense episodes was nearly the same in the B and C clusters. In the D and E, daily precipitation totals above 9 mm are evident in almost 22 and 26 % of the all-N patterns. In terms of cyclonic conditions (Fig. 8b), D and E sub-regions are more sensitive to the precipitation than the other three cluster zones. Very intense episodes are more common in the E sub-basins. Many flash floods occur during the activity of C types in this sub-basin. After transfer of more humidity and precipitation to the Aegean side of the region, the numbers of very intense

episodes decrease in the Thrace basin. Because of the distance of the cyclone centre from the north and northeast of the region, the frequencies of the intense and very intense episodes decrease compared with the other basins.

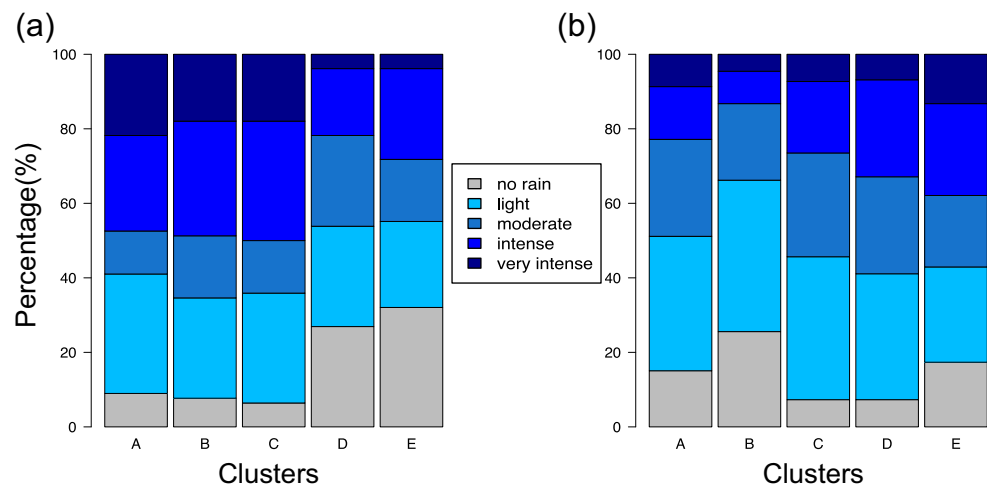
4 Summary and conclusions

In this paper, we first identified the regional patterns of precipitation in Marmara (NW Turkey) by applying the Ward's method clustering technique to the daily winter precipitation amounts. Then, we extracted the long-term composites and frequencies of atmospheric CTs and explored their contribution to daily precipitation intensity for each cluster. To identify atmospheric CTs, we used automated LWT methodology in the daily mean NCEP/NCAR reanalysis of sea level pressure data for the period from 1960 to 2012. Later, two indices (i.e. normalised relative occurrence of rainy days ($PROB_{ct}/PROB_{tot}$) and normalised relative daily amount of precipitation ($PREC_{ct}/PREC_{tot}$)) were applied to all cluster solutions to investigate the influence of CTs on the occurrence and intensity of precipitation.

As a consequence of the Ward's method, the region was divided into five main sub-regional precipitation climates: Marmara-Black Sea, Black Sea, Marmara, Thrace, and Aegean (cluster letters A, B, C, D, and E, respectively). According to the CTs results, N, NE, NW and cyclonic (C) patterns have the highest probability that rainfall will occur in the whole Marmara region. These types were also defined as the wet CTs by Baltacı et al. (2015). Additionally, $PROB_{ct}/PROB_{tot}$ results indicate that whereas the eastern part of the region concludes with precipitation during E days, western basins have rainy days during the southerly components of the patterns (S, SE, and SW).

By analysing the distribution of average precipitation intensity for each CT, it was found that the highest probability of extreme precipitation is during N and cyclonic CTs in all

Fig. 8 Percentage contribution of **a** N and **b** C synoptic weather types to the winter categories of precipitation (see Section 3.4) for five clusters.



cluster zones. As explained by Baltacı et al. (2015), type N divides the region into two parts (as east and west) with regard to precipitation intensity, and the eastern stations become remarkably wetter than others. However, the precipitation intensity index showed that west sub-regions (clusters D and E) also have the highest precipitation intensity gradients during N cases. This can be explained by intense moisture transport from the Marmara Sea. On the other hand, we found that the highest daily rainfall totals occur in the N, NW, and cyclonic (C) types in clusters D and E. During C types, almost 37 % of the daily precipitation intensities are greater than 9 mm/day in these clusters, which make affected sub-regions more sensitive to the flash flood events. Concerning eastern clusters, although the influence of NE type on rainfall magnitude is more significant, NW patterns show high precipitation intensities in all clusters of the region, except the Black Sea.

Any spatio-temporal changes in wintertime rainfall variability affect the sustainability of water management policies as well as the socioeconomic development of the region. Therefore, it is necessary to conduct more comprehensive studies based on similar sub-regional precipitation and the contribution of CTs to the different precipitation climates of sub-basins. This study is a first step in analysing the relationship between CTs and their impacts on similar precipitation climates in Marmara.

Acknowledgments We thank two anonymous reviewers for their comments and suggestions, which contributed to the improvement of this paper. We also thank Omer Yetemen for his stimulating discussions and constructive criticisms.

References

- Baltacı H, Göktürk OM, Kındap T, Ünal A, Karaca M (2015) Atmospheric circulation types in Marmara Region (NW Turkey) and their influence on precipitation. *Int J Climatol* 35:1810–1820
- Brisson E, Demuzere M, Kwakernaak B, Van Lipzig NPM (2011) Relations between atmospheric circulation and precipitation in Belgium. *Meteorol Atmos Phys* 111:27–39
- Burt TP, Ferranti EJS (2012) Changing patterns of heavy rainfall in upland areas: a case study from northern England. *Int J Climatol* 32: 518–532
- Collier GC, Krzysztofowicz R (2000) Special issue on quantitative precipitation forecast. *J Hydrol* 239:1–338
- Erinç S (1984) *Climatology and its methods*. Güraç Press Inc., Istanbul
- Fovell RG, Fovell MC (1993) Climate zones of the conterminous United States defined using cluster analysis. *J Clim* 6:2103–2135
- Gallego MC, Garcia JA, Vaquero JM, Mateos VL (2006) Changes in frequency and intensity of daily precipitation over the Iberian Peninsula. *J Geophys Res* 111:D24105
- Gong X, Richman MB (1995) On the application of cluster analysis to growing season precipitation data in North America east of the Rockies. *J Clim* 8:897–931
- Goodess CM, Jones PD (2002) Links between circulation and changes in the characteristics of Iberian rainfall. *Int J Climatol* 22:1593–1615
- Huth R, Beck C, Philipp A, Demuzere M, Ustrnul Z, Cahynova M, Kysely J, Tveito OE (2008) Classifications of atmospheric circulation patterns. *Ann N Y Acad Sci* 1146:105–152
- Jenkinson AF, Collison FP (1977) An initial climatology of gales over the North Sea. Synoptic Climatology Branch Memorandum 62, Meteorological Office: Bracknell, UK.
- Jones PD, Hulme M, Briffa KR (1993) A comparison of Lamb circulation types with an objective classification scheme. *Int J Climatol* 13:655–663
- Kalnay E, Kanamitsu M, Kistler R, Collins W, Deaven D, Gandin L, Iredell M, Saha S, White G, Wollen J, Zhu Y, Chelliah M, Ebisuzaki W, Higgins W, Janowiak J, Mo KC, Ropelewski C, Wang J, Leetmaa A, Reynolds R, Jenne R, Joseph D (1996) The NCEP/NCAR 40-year reanalysis project. *Bull Am Meteorol Soc* 77: 437–471
- Lopez-Bustins J, Martin-Vide J, Sanchez-Lorenzo A (2008) Iberia winter rainfall trends based upon changes in teleconnection and circulation patterns. *Glob Planet Chang* 63:171–176
- Ning L, Bradley RS (2015) Winter precipitation variability and corresponding teleconnections over the northeastern United States. *J Geophys Res Atmos* 113:7931–7945
- Osborn TJ, Hulme M (2002) Evidence for trends in heavy rainfall events over the UK. *Phil Trans R Soc A* 360:1313–1325
- Osborn TJ, Hulme M, Jones PD, Basnett TA (2000) Observed trends in the daily intensity of United Kingdom precipitation. *Int J Climatol* 20:347–364
- Philipp A, Bartholy J, Beck C, Erpicum M, Esteban P, Fettweis X, Huth R, James P, Jourdain S, Kreienkamp F, Krennert T, Lykoudis S, Michalides SC, Pianko-Kluczynska K, Post P, Rasilla Alvarez D, Schiemann R, Spekat A, Tymvios FS (2010) Cost733cat—a database of weather and circulation type classifications. *Phys Chem Earth* 35:360–373
- Sahin S, Cigizoglu HK (2012) The sub-climate regions and the sub-precipitation regime regions in Turkey. *J Hydrol* 450–451:180–189
- Sönmez İ, Kömüşcü AÜ (2011) Reclassification of rainfall regions of Turkey by K-means methodology and their temporal variability in relation to North Atlantic Oscillation (NAO). *Theor Appl Climatol* 106:499–510
- Türkeş M (1996) Spatial and temporal analysis of annual rainfall variations in Turkey. *Int J Climatol* 16:1057–1076
- Türkeş M, Tatlı H (2011) Use of the spectral clustering to determine coherent precipitation regions in Turkey for the period 1929–2007. *Int J Climatol* 31:2055–2067
- Ünal Y, Kındap T, Karaca M (2003) Redefining the climate zones of Turkey using cluster analysis. *Int J Climatol* 23:1045–1055